NUCL SCI TECH (2017) 28:159
DOI 10.1007/s41365-017-0307-7

FEA-based structural optimization design of a side cooling collimating mirror at SSRF

Li-Min Jin[1] · Na-Xiu Wang[1] · Wan-Qian Zhu[1] · Feng-Gang Bian[1] · Zhong-Min Xu[1]

Received: 10 April 2017 / Revised: 7 June 2017 / Accepted: 11 June 2017 / Published online: 26 October 2017

Abstract Based on finite element analysis of thermal mechanical behavior, structural optimization design was proposed for a side cooling collimating mirror subjected to high heat load for a beamline at SSRF (Shanghai Synchrotron Radiation Facility). The temperature distribution, stress concentration effect, maximum equivalent (von-Mises) stress, and slope error of the mirror were analyzed. In particular, the cooling water channels of the traditional structural design were optimized, and the modified designs were further optimized. Although the traditional structural and the improved designs could meet requirements for the temperature and thermal stress, the deformation gradients were relatively large for several structural designs, and this led to larger slope error. The further improved structural designs could be of better performance.

Keywords Finite element analysis (FEA) · Synchrotron radiation · Heat load · Structural optimization

1 Introduction

A third-generation light source is advantageous in its high brightness and flux, wide energy spectrum, and high collimation, and is widely used in physics, chemistry, biology, medicine, archeology, materials science, microelectronics, environmental protection etc. As an advanced scientific facility, with long-term stability and high-quality operation of the beamlines, it brings great convenience for researchers all over the world [1–5]. As a critical influencing factor on high-quality operation of the light source, the optical systems play an important role. And as one of the primary elements in the optical systems, the various optical mirrors (deflection, focusing, harmonic rejection, collimating etc.), made of single-crystal silicon mostly, affect optical performance of the beamlines [6–9] by their surface topography and slope error.

During the long-term operation, the cumulative thermal effect induces slight local deformation of lattice on the crystal surface, thus affecting the beamline quality [10–15]. Finite element analysis (FEA) has been performed to predict the thermodynamic behavior of mirror prototypes, which undergo high heat loading conditions. FEA has also been applied to design the better mirror structures for effectively reducing the negative thermal deformation. The numerical calculations are conducted throughout the structural designs until the mirrors satisfy the engineering requirements [16–20].

The radioactive materials beamline in Phase II beamline project of SSRF (Shanghai Synchrotron Radiation Facility) will be dedicated to meet the research requirements of nuclear power in China, for studies on nuclear fuel fabrication, spent fuel reprocessing, and structural and functional materials for nuclear reactors, environmental radioactive contamination etc. The beamline will provide advanced analytical tools of XAS, XRD, XRF, imaging, and associated microcharacterization techniques for analyzing radioactive samples, and for applications in other research fields. The beamline uses a cylindrical mirror to collimate the light beam in the vertical direction, thus to

The work is supported by the National Natural Science Foundation of China (No. 11175243).

✉ Zhong-Min Xu
xuzhongmin@sinap.ac.cn

1 Shanghai Institute of Applied Physics, Chinese Academy of Sciences, Shanghai 201204, China

improve the energy resolution and luminous flux. For the scientific design requirements of the collimating mirror, the meridional slope error (RMS) should be less than 1.5 μrad. In particular, the meridional slope error (RMS) caused by heat load should be less than 1 μrad.

In this paper, thermal mechanical behavior of a side cooling collimating mirror for the radioactive materials beamline is analyzed by FEA. The temperature distribution, stress concentration effect, maximum equivalent (von-Mises) stress, and slope error are studied. To meet the design requirements of the beamline, the mirror structural designs are optimized in series and the results are compared, such as modifying the designs by adjusting the water channel length, and improving the modified designs by optimizing the cut-off region for water channels. Such an effort can be extended to designing other types of optical mirrors subjected to high heat load.

2 Finite element model

The FEA was performed by using the commercial finite element software ANSYS WORKBENCH (Version: 14.5) and windows XP platform.

2.1 Geometry model

Figure 1a shows the 3-D model of the side cooling collimating mirror system, which includes one mirror and two cooling water channels. Owing to the principle of symmetry, as shown in Fig. 1b, only half of the system is established to perform FEA. The mirror is made of single-crystal silicon attached to the cooling copper block. The cooling medium is deionized water. According to traditional design, the contact length of the mirror to the copper block equals to the mirror's length.

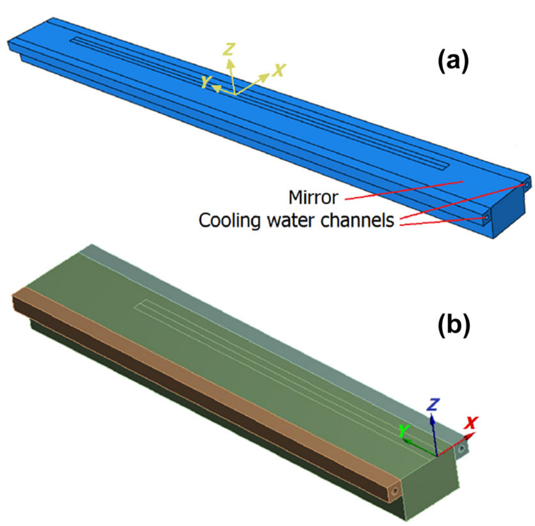

Fig. 1 The side cooling collimating mirror **a** 3-D model **b** 1/2 FEA model

The material parameters are listed in Table 1. The mirror is sized at 80 mm (*X*) × 1200 mm (*Y*) × 55 mm (*Z*). The square cooling water tube is 20 mm (*X*) × 1200 mm (*Y*) × 20 mm (*Z*). The circular cooling water channel is 8 mm in diameter.

2.2 Interaction condition

Considering the existence of slight relative displacement at the contact area between the mirror and copper block under high heat load, the interaction property was set at No Separation. As indium foil was used as the interstitial material between the silicon and copper in practical engineering operation, the thermal conductance coefficient was set at 3000 W m^{-2} °C^{-1} [21].

2.3 Boundary and loading conditions

As shown in Fig. 2a, b, the heat load was in the central specific area of the mirror, and symmetry constraint was imposed on the symmetry planes. The power density distribution on the mirror is shown in Fig. 2c. The peak power density was 10.24 kW/$mrad^2$. The horizontal and the vertical emission angles of the light beam were 1 and 0.12 mrad, respectively. The beam was at a grazing incidence angle of 2.4 mrad on the working surface of mirror. The distance between the mirror and the light source was 19 m. And the absorption efficiency of the mirror was 21.74%. It can be calculated that the maximum heat power absorbed by the mirror was 240.7 W. The size of footprint (synchrotron radiation area) was 19 mm (*X*) × 950 mm (*Y*). From Eqs. (1–5) and computational conservatism of FEA, the calculated equivalent convective heat transfer coefficient was $h = 3000$ W m^{-2} °C^{-1}, while the initial reference temperature was 30 °C.

$$h = kNu/\mathrm{D}, \tag{1}$$

$$Nu = 0.023Re^{0.8}Pr^{0.4}, \tag{2}$$

$$Re = \rho vD/\mu, \tag{3}$$

$$Pr = \mu C_{\mathrm{p}}/k, \tag{4}$$

$$h = 0.023\rho^{0.8}v^{0.8}C_{\mathrm{p}}^{0.4}k^{0.6}/\left(\mu^{0.4}D^{0.2}\right), \tag{5}$$

where h is the convective heat transfer coefficient; Nu is the Nusselt coefficient; k is the thermal conductivity of the cooling medium; D is the diameter of the circular cooling tube; Re is the Reynolds number, reflecting the effect of convective strength on heat transfer; Pr is the Prandtl number, reflecting the effect of fluid properties; ρ is the density, v is the velocity, μ is the viscosity, and C_{p} is specific heat of the cooling medium.

Table 1 Mechanical parameters of materials

Materials	Density (kg m^{-3})	Elastic modulus (GPa)	Poisson's ratio	Yield stress (MPa)	Thermal conductivity (W m^{-1} °C^{-1})	Thermal expansion coefficient (°C^{-1}), 25 °C
Silicon	2329	112.40	0.28	120.00	148.00	2.50×10^{-6}
Copper	8900	110.00	0.34	220.00	391.00	1.75×10^{-5}

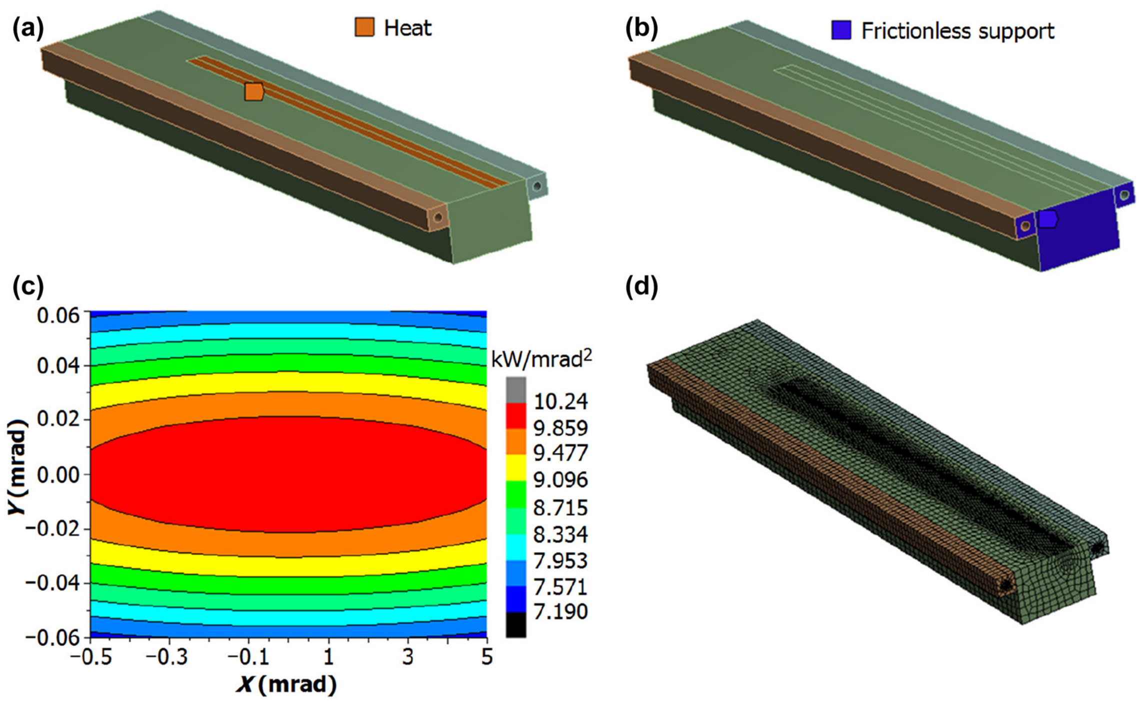

Fig. 2 FEA settings of the loading (**a**) and boundary (**b**) conditions, the power density distribution (**c**) and the mesh (**d**)

2.4 Mesh scheme

As shown in Fig. 2d, for the FEA model, all parts were assigned to global seeds in element size of 8 mm and meshed with the technique of hex-dominated method [22]. In particular, for the critical synchrotron radiation area subjected to high heat load, the finer element size of 2 mm was used. The entire model had 200,292 nodes and 50,629 elements.

3 Results and discussions

3.1 Temperature and thermal stress distribution

Temperature and thermal stress are critical indicators for optical mirrors subjected to high heat load. The mirrors work properly when the two parameters are within the normal operating range. The temperature distribution of the mirror is shown in Fig. 3a, the relative high temperature located at the synchrotron radiation area subjected directly to the high heat load, with the maximum temperature of 36 °C, which was within the normal operating temperature range of single-crystal silicon. Figure 3b shows the equivalent (von-Mises) thermal stress distribution of FEA model. The maximum equivalent thermal stress located at the synchrotron radiation area, with the maximum thermal stress of 0.3 MPa, which was also within the normal thermal stress range of single-crystal silicon (Table 1).

3.2 Slope error

Slope error is a key technical factor of synchrotron radiation optical mirrors, indicating optical surface performance of the mirrors subjected to high heat load. Figure 4a shows the tangential deformation contour along the central line of the synchrotron radiation area. It can be seen that the deformation changed continuously along the meridian direction of mirror. The deformation maximized in the central part of the mirror and decreased gradually

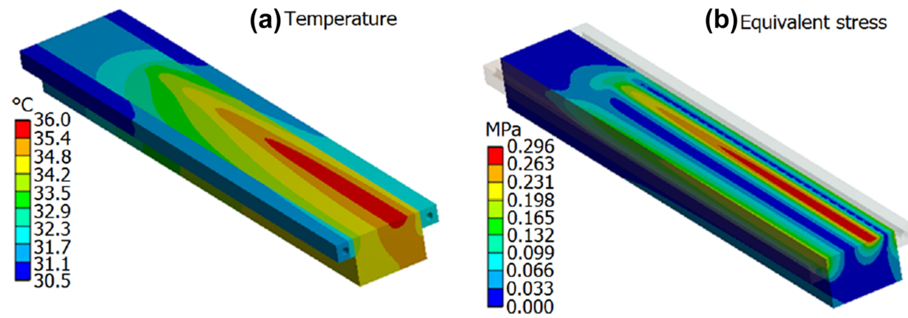

Fig. 3 Temperature (**a**) and stress (**b**) distributions of the FEA model

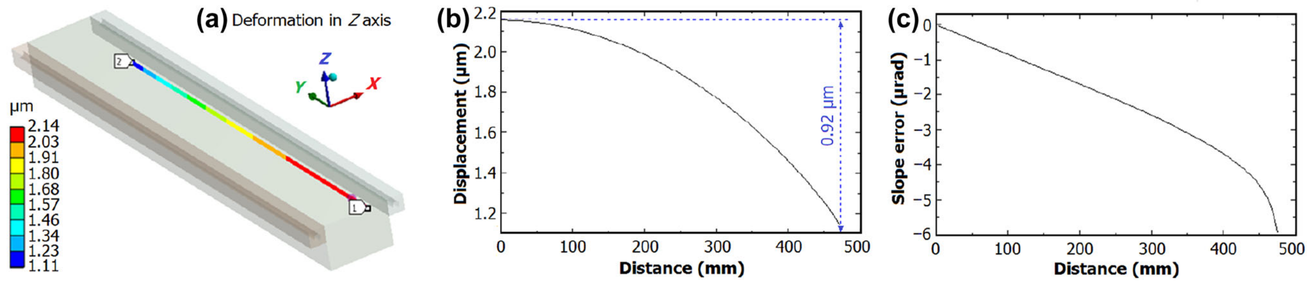

Fig. 4 Tangential deformation of synchrotron radiation area. **a** contour **b** deformation along the meridian direction **c** the slope error

along both sides. Such phenomenon was related to the distribution of the heat load which was applied at this specific region. Figure 4b shows the tangential deformations of the synchrotron radiation area along meridian direction. In Fig. 4c showing the slope errors, however, the RMS value of slope error was 2.6 μrad, while the design requirements of the mirror are less than 1 μrad.

3.3 Modified design and simulation results

A modified design was proposed to improve the slope error. As shown in Fig. 4, the gradient of deformation was relatively large along the meridian direction from the center to the edge of synchrotron radiation area, i.e., the maximum difference in deformation was 0.92 μm, which was the main reason leading to the large slope error. Take the structural design of long cooling system into consideration, it caused the relatively large temperature gradient at the specific region; thus, it was dominantly contributed to the phenomenon described above. To reduce this kind of negative effect, a series of short cooling systems were designed, as shown in Fig. 5a. In new designs, the length of modified square cooling water channels were 1080, 900, 800, 780, 760 and 740 mm, respectively, without changing the other sizes.

Based on the modified models, a series of FEA was performed. Figure 5b, c show the maximum temperature and maximum thermal stress as a function of the channel length (from 700 to 1200 mm of the original design), respectively. It can be seen that although the maximum temperature increased at shorter channel lengths, they were still within the normal operating range of silicon. The maximum stress values were almost kept around 0.3 MPa, which was also within the normal operating range of silicon.

As shown in Fig. 5d,e, the gradient of tangential deformation of the modified designs was significantly less than that of the original one. In addition, the modified design of 760 mm channel length had the smallest gradient in normal deformation, while the maximum difference in deformation for the modified model was approximately 0.16 μm, which was only 17.4% of that of the original model (0.92 μm). The RMS value of slope error was 0.91 μrad, which was only 35% of that of the original model (2.6 μrad). This slope error was far less than that of the original design.

3.4 Further improved design and simulated results

To further improve the mirror performance, other improved structures for cooling system were designed. In Fig. 5d, it can be found that the segment of 50–300 mm was the critical region for the optimization, with the smallest deformation and hence reduced difference in deformation. So, even better results can be obtained by optimal designs for this specific region.

According to Sect. 3.3, the channel length of 760 mm is of the best cooling effect. For further improving cooling structure, four types of 760 mm cooling water channels were designed (Fig. 6a). Each design had a segment

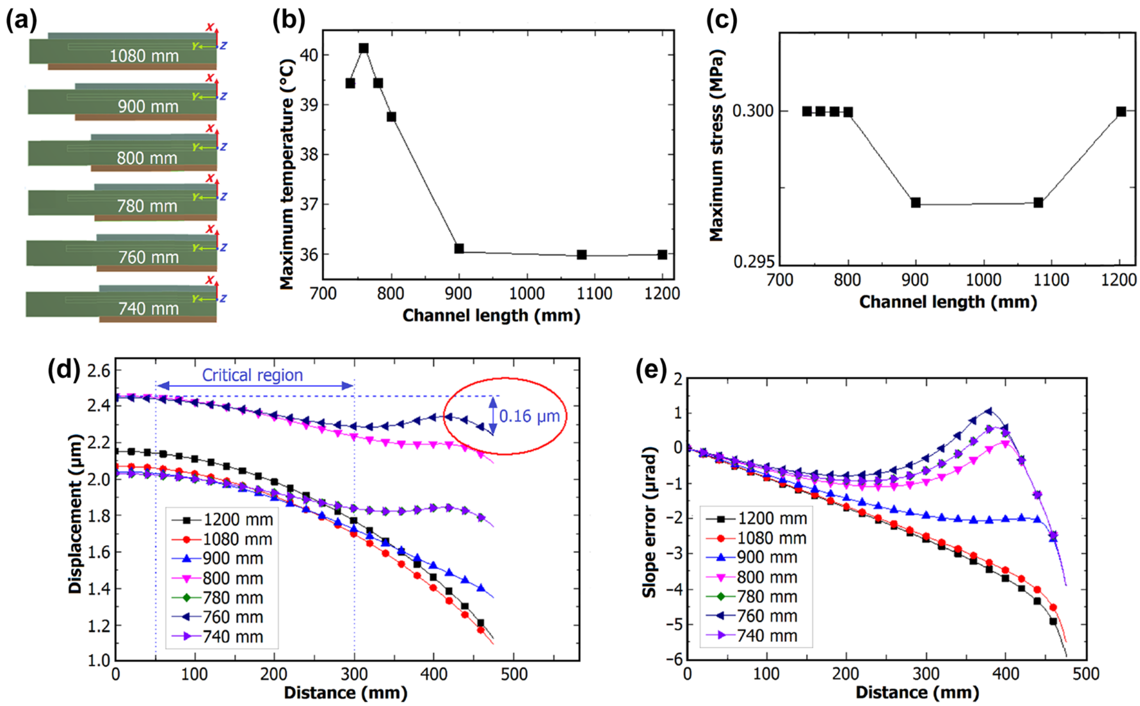

Fig. 5 Modified FEA models of different channel lengths (**a**); maximum temperature (**b**), maximum thermal stress (**c**), tangential deformation (**d**) and slope error (**e**), as a function of channel length. The tangential deformation was optimized in the critical region

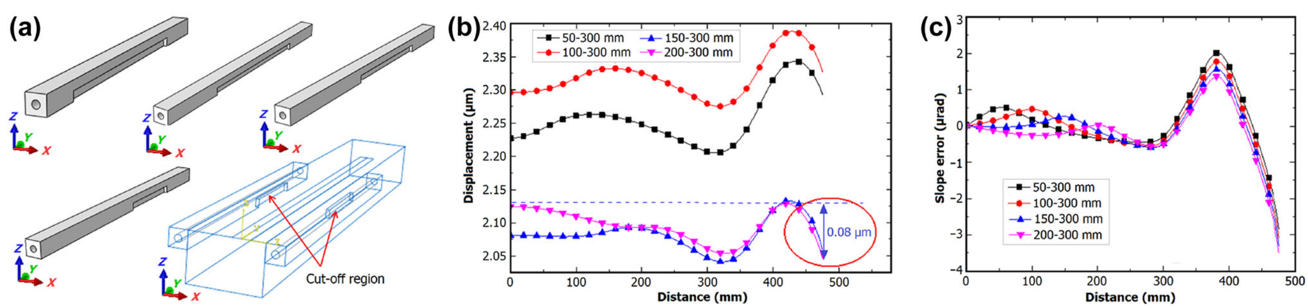

Fig. 6 Four types of structural optimization design schemes (**a**) for cooling water channels, segment removal of 50–300, 100–300, 150–300, or 200–300 mm regions, with the cut-off width of 4 mm and height of 10 mm; the tangential deformation (**b**) and slope error (**c**) of the further improved designs as a function of the distance

removal for the cooling channel at the specific region. The cut-off regions were 50–300, 100–300, 150–300 or 200–300 mm, with the cut-off width of 4 mm and height of 10 mm.

Figure 6b, c show the tangential deformation and slope error for the further improved designs, respectively. One sees that the maximum gradient of normal deformation of the model with the cut-off region of 200–300 mm was approximately 0.08 μm, which was only 50% of that of the original optimized model (0.16 μm), hence the smallest gradient in tangential deformation. Furthermore, the calculated RMS value of slope error was 0.77 μrad, being 84.6% of that of the original optimized model (0.91 μrad), and 77% of the beamline requirement (1 μrad). Therefore, the further improved model with the cut-off region of 200–300 mm shall be pretty good.

4 Conclusion

The thermal mechanical behavior and structural optimization designs of a side cooling reflection mirror subjected to high heat load (240.7 W) in synchrotron radiation were proposed based on FEA. By optimizing the length of the cooling water channels, the temperature distribution, stress concentration effect, maximum equivalent stress, as well as slope error of the mirror, were analyzed by comparing the results between the traditional structural design and the modified designs, and the following conclusions have been obtained:

1. Temperature and thermal stress are critical important technical indicators for optical mirrors subjected to high heat load; the optical mirrors may work properly while both of them are within the normal operating range. For the temperature and thermal stress, the proposed methods can meet the design requirements.
2. For the traditional structural design, it can be found that the gradient of tangential deformation was relatively large along the meridian direction, when leading to the large slope error of reflection mirror. Take the structural design of long cooling system into consideration, it caused the relatively larger temperature gradient at the specific synchrotron radiation region; thus, it was dominantly contributed to the phenomenon above. In order to reduce the negative effect, a new short cooling system was designed for the modified structure.
3. Slope error can directly indicate the optical surface performance of mirrors subjected to high heat load. For the traditional structural design, the RMS value of slope error was 2.6 μrad, which cannot meet the design requirements. As for the modified structural design, the calculated RMS value of slope error was 0.91 μrad, which was far less than the original design result.
4. To further improve the performance of the mirror, the further improved structural designs of cooling system were recommended. Four types of new designs for cooling channels were designed. It was found that the maximum gradient of tangential deformation for the further improved model with the cut-off region of 200–300 mm was 0.08 μm, which was only 50% of that of the original optimized model (0.16 μm); thus, it indicated the smallest gradient in tangential deformation. Furthermore, the calculated RMS value of slope error was 0.77 μrad, which was 84.6% of that of the original optimized model (0.91 μrad), and 77% of the beamline requirement (1μrad).

References

1. C. Kunz, Synchrotron radiation: third generation sources. J. Phys. Condens, Mater. **13**, 7499–7510 (2001). doi:10.1088/0953-8984/13/34/303
2. S. Ferrer, Y. Petroff, Surface science done at third generation synchrotron radiation facilities. Surf. Sci. **500**, 605–627 (2002). doi:10.1016/S0039-6028(01)01584-9
3. T.A. Ezquerra, M.C. Garcia-Gutierrez, A. Nogales et al., Introduction to the special issue on “Applications of synchrotron radiation in polymers science”. Eur. Polym. J. **81**, 413–414 (2016). doi:10.1016/j.eurpolymj.2016.05.002
4. F. Chen, F. Mao, Z.N. Chen et al., Application of synchrotron radiation X-ray computed tomography to investigate the agglomerating behavior of TiB_2 particles in aluminum. J. Alloys Compd. **622**, 831–836 (2015). doi:10.1016/j.jallcom.2014.10.190
5. Z.L. Shi, S.H. Zhou, S. Fu, Potential applications of synchrotron radiation to the treatment of cancer. Nucl. Sci. Tech. **24**, 010101 (2013). doi:10.13538/j.1001-8042/nst.2013.01.006
6. C.A. Liu, G.E. Ice, W. Liu et al., Fabrication of nested elliptical KB mirrors using profile coating for synchrotron radiation X-ray focusing. Appl. Surf. Sci. **258**, 2182–2186 (2012). doi:10.1016/j.apsusc.2011.02.079
7. S.J. Chen, C.K. Kuan, S.Y. Perng et al., New focusing mirror system for synchrotron radiation infrared beamlines. Opt. Eng. **43**, 3077–3082 (2004). doi:10.1117/1.1813438
8. M.R. Howells, Some fundamentals of cooled mirrors for synchrotron radiation beam lines. Opt. Eng. **35**, 1187–1197 (1996). doi:10.1117/1.600607
9. J. Susini, Design parameters for hard X-ray mirrors the European synchrotron-radiation facility case. Opt. Eng. **34**, 361–376 (1995). doi:10.1117/12.194835
10. S.N. Qian, W. Jark, G. Sostero et al., Precise measuring method for detecting the in situ distortion profile of a high-heat-load mirror for synchrotron radiation by use of a pentaprism long trace profiler. Appl. Opt. **36**, 3769–3775 (1997). doi:10.1364/AO.36.003769
11. P.H. Mui, G. Srajer, D.M. Mills, *In situ* surface monitoring system for synchrotron mirrors under high heat load. Appl. Opt. **36**, 5546–5551 (1997). doi:10.1364/AO.36.005546
12. P. Carpentier, M. Rossat, P. Charrault et al., Synchrotron monochromator heating problem, cryogenic cooling solution. Nucl. Instrum. Methods A **456**(3), 163–176 (2001). doi:10.1016/S0168-9002(00)00578-7
13. A.I. Chumakov, I. Sergeev, J.P. Celse et al., Performance of a silicon monochromator under high heat load. J. Synchrotron Radiat. **21**, 315–324 (2014). doi:10.1107/S1600577513033158
14. Z.M. Xu, N.X. Wang, An optimized side-cooling scheme for a collimation mirror at the SSRF. J. Synchrotron Radiat. **19**, 428–430 (2012). doi:10.1107/S0909049512004050
15. N.X. Wang, S.L. Liu, Z.M. Xu et al., Cooling of double crystal monochromator with sagittal focus at SSRF. Nucl. Sci. Tech. **21**, 65–68 (2010). doi:10.13538/j.1001-8042/nst.21.65-68
16. L. Zhang, M.S. Del Rio, G. Monaco et al., Thermal deformation of cryogenically cooled silicon crystals under intense X-ray beams: measurement and finite-element predictions of the surface shape. J. Synchrotron Radiat. **20**, 567–580 (2013). doi:10.1107/S0909049513009436
17. X.C. Cheng, L. Zhang, C. Morawe et al., Thermal stress prediction in mirror and multilayer coatings. J. Synchrotron Radiat. **22**, 317–327 (2015). doi:10.1107/S1600577514026009
18. A.K. Sinha, Heat transfer studies for a crystal in a synchrotron radiation beamline. Sadhana-Acad. P. Eng. S. **34**, 243–254 (2009)
19. L. Zhang, R. Barrett, P. Cloetens et al., Anisotropic elasticity of silicon and its application to the modelling of X-ray optics. J. Synchrotron Radiat. **21**, 507–517 (2014). doi:10.1107/S1600577514004962
20. L. Zhang, W.K. Lee, M. Wulff et al., The performance of a cryogenically cooled monochromator for an in-vacuum undulator beamline. J. Synchrotron Radiat. **10**, 313–319 (2003). doi:10.1107/S0909049503012135
21. A.M. Khounsary, D. Chojnowski, L. Assoufid et al., Thermal contact resistance across a copper-silicon interface. Proc. SPIE **3151**, 45–51 (1997). doi:10.1117/12.294497
22. ANSYS Inc, ANSYS® Workbench ™, Release 14.5, Help System, Theory Reference for ANSYS and ANSYS Workbench. (2007)